AD-A118 430 ARMY MISSILE COMMAND REDSTONE ARSENAL AL RESEARCH D--ETC F/G 20/6
MULTIPLEX HOLOGRAPHIC FILTERING THROUGH CONTACT SCREENS.(U)
FEB 82 J C DUTHIE, H K LIU

UNCLASSIFIED DRSMI/RR-82-7-TR SRI-AD-F950 270 NL

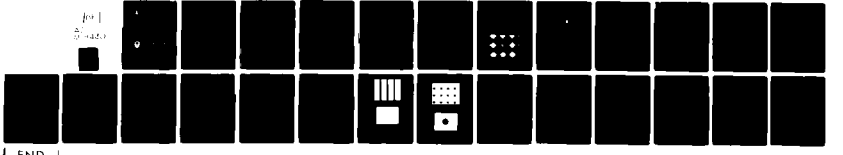

END
DATE FILMED
09-82
DTIC

TECHNICAL REPORT RR-82-7

MULTIPLEX HOLOGRAPHIC FILTERING THROUGH CONTACT SCREENS

J. C. Duthie and H. K. Liu
Research Directorate
US Army Missile Laboratory

8 February 1982

U.S. ARMY MISSILE COMMAND
Redstone Arsenal, Alabama 35809

Approved for public release; distribution unlimited.

DISPOSITION INSTRUCTIONS

DESTROY THIS REPORT WHEN IT IS NO LONGER NEEDED. DO NOT RETURN IT TO THE ORIGINATOR.

DISCLAIMER

THE FINDINGS IN THIS REPORT ARE NOT TO BE CONSTRUED AS AN OFFICIAL DEPARTMENT OF THE ARMY POSITION UNLESS SO DESIGNATED BY OTHER AUTHORIZED DOCUMENTS.

TRADE NAMES

USE OF TRADE NAMES OR MANUFACTURERS IN THIS REPORT DOES NOT CONSTITUTE AN OFFICIAL INDORSEMENT OR APPROVAL OF THE USE OF SUCH COMMERCIAL HARDWARE OR SOFTWARE.

UNCLASSIFIED

SECURITY CLASSIFICATION OF THIS PAGE (When Data Entered)

REPORT DOCUMENTATION PAGE		READ INSTRUCTIONS BEFORE COMPLETING FORM
1. REPORT NUMBER RR-82-7	2. GOVT ACCESSION NO. AD-A118 430	3. RECIPIENT'S CATALOG NUMBER
4. TITLE (and Subtitle) MULTIPLEX HOLOGRAPHIC FILTERING THROUGH CONTACT SCREENS		5. TYPE OF REPORT & PERIOD COVERED 6. PERFORMING ORG. REPORT NUMBER
7. AUTHOR(s) J. G. Duthie and H. K. Liu		8. CONTRACT OR GRANT NUMBER(s)
9. PERFORMING ORGANIZATION NAME AND ADDRESS Commander, US Army Missile Command ATTN: DRSMI-RR Redstone Arsenal, AL 35898		10. PROGRAM ELEMENT, PROJECT, TASK AREA & WORK UNIT NUMBERS
11. CONTROLLING OFFICE NAME AND ADDRESS Commander, US Army Missile Command ATTN: DRSMI-RPT Redstone Arsenal, AL 35898		12. REPORT DATE 8 Feb 82 13. NUMBER OF PAGES 23
14. MONITORING AGENCY NAME & ADDRESS(if different from Controlling Office)		15. SECURITY CLASS. (of this report) UNCLASSIFIED 15a. DECLASSIFICATION/DOWNGRADING SCHEDULE

16. DISTRIBUTION STATEMENT (of this Report)

Approved for public release; distribution unlimited.

17. DISTRIBUTION STATEMENT (of the abstract entered in Block 20, if different from Report)

18. SUPPLEMENTARY NOTES

19. KEY WORDS (Continue on reverse side if necessary and identify by block number)

Optics
Optical Data Processing
Holography
Missile Guidance
Correlators

20. ABSTRACT (Continue on reverse side if necessary and identify by block number)

The basic principle of applying a specific contact screen for performing multiplex holographic filtering in a real-time coherent optical correlator is described. The specific design and fabrication of a one-dimensional and a two-dimensional gray density contact screen are described. The two-dimensional screen can yield nearly a 5 x 5 array of spectra islands in a coherent image processor.

DD FORM 1 JAN 73 1473 EDITION OF 1 NOV 65 IS OBSOLETE

UNCLASSIFIED

SECURITY CLASSIFICATION OF THIS PAGE (When Data Entered)

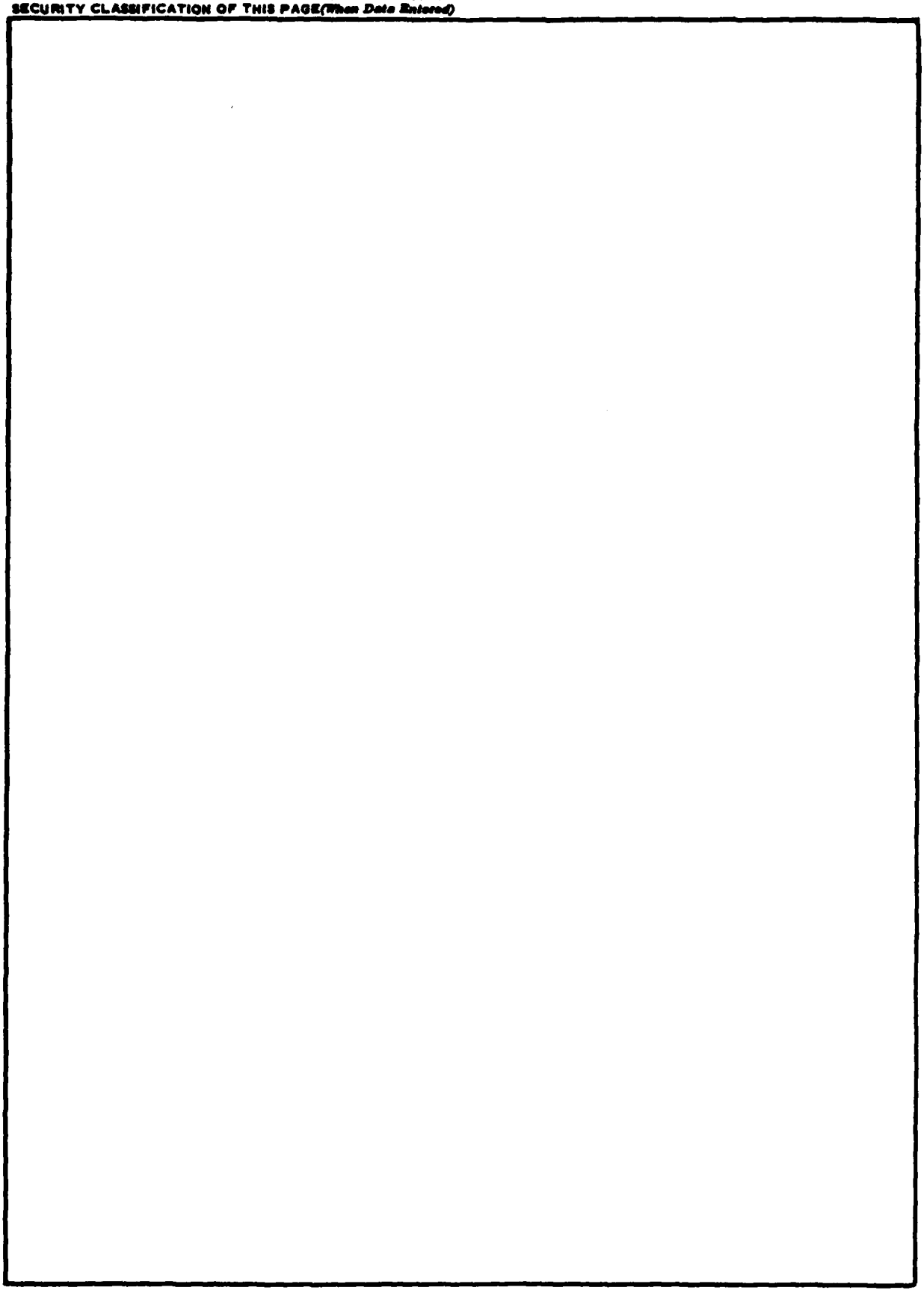

CONTENTS

I. INTRODUCTION

Optical holographic matched filter correlators[1] can potentially be used for dynamic pattern recognition such as in automatic aerial reconnaisance data[2] interrogation and missile guidance for tactical homing applications.[3] The main problem which must be resolved before the technique can be used in these applications is the storage capacity of the filter and the effectiveness of the detection of the output of the correlation. Recently, Leib, et al.[2-4] designed an optically matched filter correlation system in which a large array of holograms can be stored in a matched filter through the use of a multiple number of holographic lenses. They theoretically predicted that the system has a possible storage capacity of 2500 matched filters of an M-60 tank per square centimeter. Experimental demonstration of this capacity has not yet been reported. The purpose of this report is to present a new and different method for making matched filters that are capable of storing multiple images and making proper pattern recognition.

II. BASIC PRINCIPLES

A. Recording of the Holographic Matched Filter

The basic idea of the new method is to record the zero-order Fourier-transformed holographic image one at a time at each of an array of locations at the Fourier plane (or matched filter plane) shown in the system[5,6] of Figure 1. The center locations of each hologram are determined according to the center of the spectra islands of the Fourier transform of a contact screen.[7]

---

[1]A. Vander Lugt and F. B. Rotz, "The Use of Film Nonlinearities in Optical Spatial Filtering," Appl. Opt. 9, 215 (1970).

[2]K. G. Leib, et al., "Optical Matched Filtering Techniques for Automatic Interrogation of Aerial Reconnaissance Film," Final Report, Contract DAAG53-75-C-0199, AD No. A030574, September 1976.

[3]K. G. Leib, et al., "Analysis of an Optically Matched Filter Guidance System for Tactical Homing Applications," Paper presented at AIAA/NASA Conference on Smart Sensors, Langley Research Center, Hampton, Virginia, November 1978.

[4]K. G. Leib, R. A. Bondurant, and M. R. Wohlers, "Optical Matched Filter Correlation Memory Techniques and Storage Capacity," Opt. Engr., 19, 414 (1980).

[5]B. D. Guenther, C. R. Christensen, and Juris Upatnieks, "Coherent Optical Processing: Another Approach," IEEE J. Quantum Electronics, QE-15, 1348, (1979).

[6]J. G. Duthie, Juris Upatnieks, C. R. Christensen, and R. D. McKenzie, Jr., "Real-Time Optical Correlation with Solid-State Sources," SPIE 213, International Computing Conference, 281 (1980).

[7]H. K. Liu, "Halftone Screen with Cell Matrix," U. S. Patent No. 4188225, February 1980.

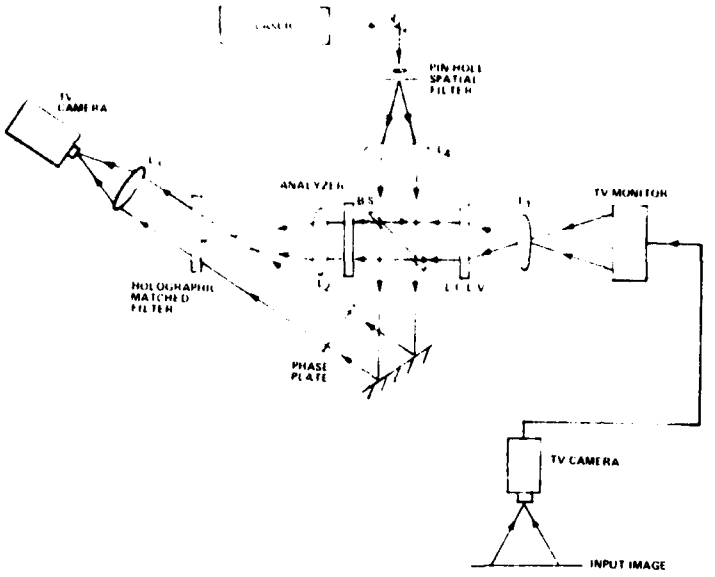

Figure 1. A real-time coherent optical correlator.

For example, a photomicrograph of the density distribution of a few cell-patterns of a contact screen is shown in Figure 2. The Fourier transform of the screen through a lens of a focal length of 30 inches is shown in Figure 3.

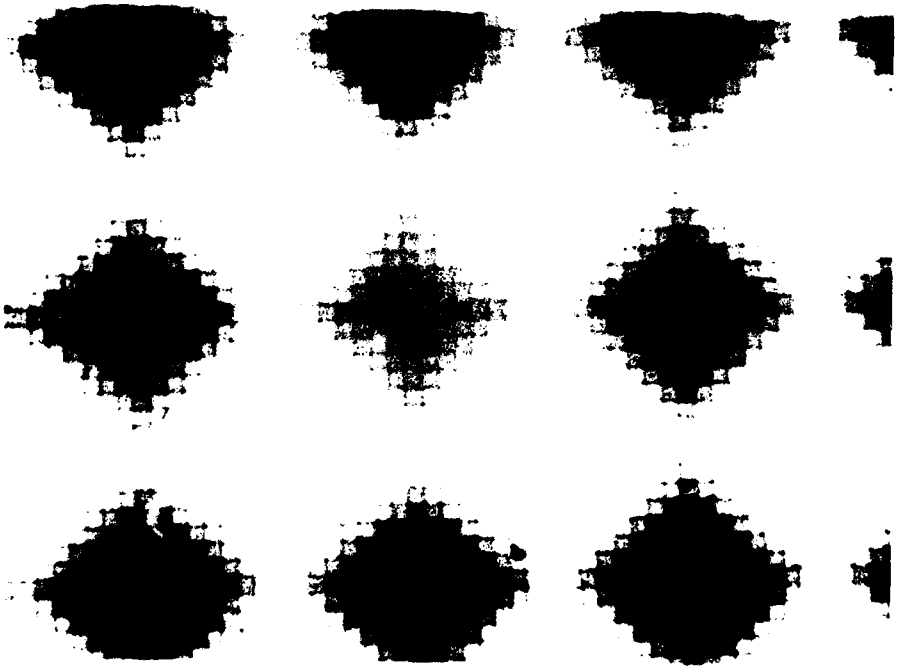

Figure 2. A photomicrograph of a few cell patterns of a 50 lines/inch contact screen.

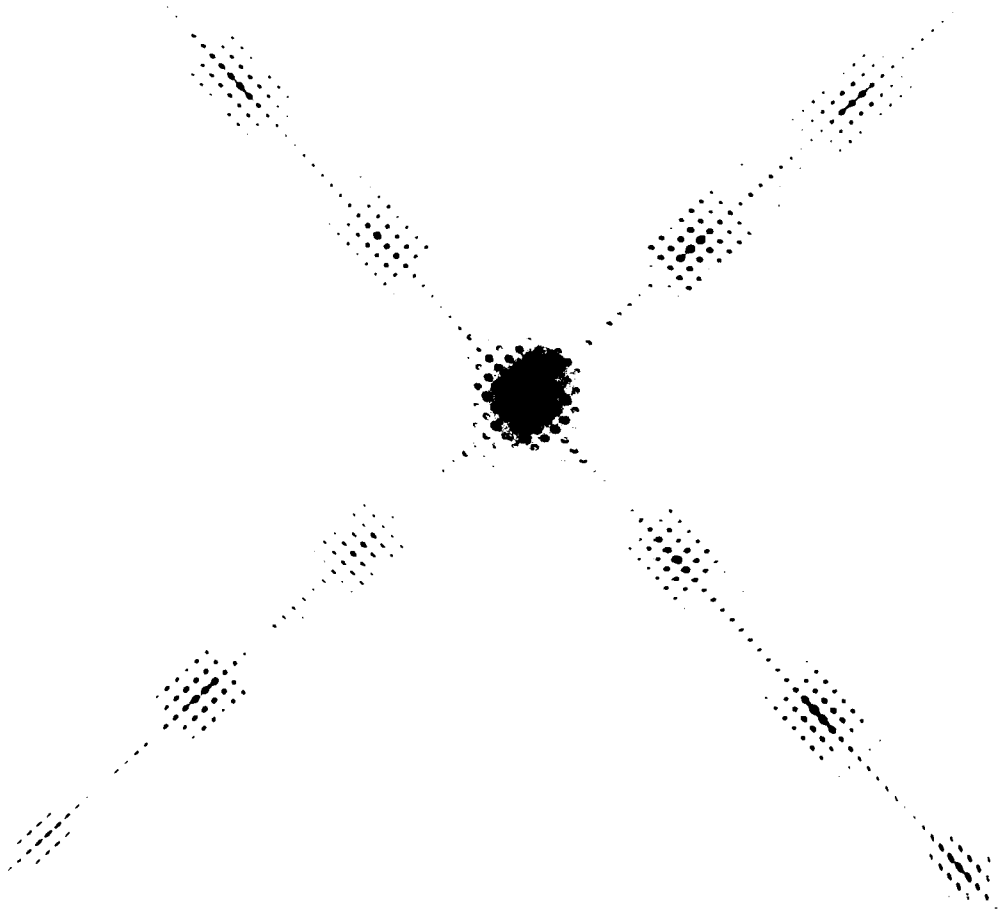

Figure 3. A photograph showing the spectra of the contact screen of Figure 1.

B. Auto-correlation Experiment

In the auto-correlation experiment, the above-recorded holographic-matched filter should be replaced at the filter plane and the contact screen should be inserted in front of the Fourier transform lens L_2 in the system as shown in Figure 1. The incoming image is diffracted by the contact screen to all the locations of the spectra islands similar to those as shown in Figure 3. If the input image is matched with any one of the images that are stored by one of the spectra islands, then an auto-correlation signal can be detected.

III. DESIGN OF A SPECIFIC CONTACT SCREEN FOR MULTIPLE-IMAGE STORAGE IN HOLOGRAPHIC-MATCHED FILTERS

The contact screen with cell patterns shown in Figure 2 is given only as an example to illustrate the idea that the screen may be utilized to achieve the purpose of multiple-image storage in a holographic-matched filter. From the pattern of the spatial spectra of the screen at the Fourier plane as shown in Figure 3, it can obviously be seen that the screen has two major drawbacks for this specific application: 1) The spectra islands are not of the same intensity, i.e., the intensity distribution among the various diffraction orders is not uniform. 2) There are perhaps too many high order terms in the spectra that may not be needed due to the finite aperture of the system. These excessive diffraction orders tend to share the total energy and reduce the light efficiency.

In order to eliminate these drawbacks of the screen in the correlation applications, a contact screen needs to be specifically designed and fabricated. The design, fabrication, and usage of a specific contact screen for the real-time correlator application is presented below.

A. Design of the Specific Screen

The goal of the design is to have a screen that can create a 5 x 5 array of spectra islands centered at the zero order of the Fourier transform plane of the lens when it is placed at the front focal plane of a lens and illuminated by a collimated beam of light. Ideally, each island in the 5 x 5 square array should approximately possess the same magnitude of light intensity and none of the input light should be diffracted to any higher order terms. Screens with one-dimensional transmittance distribution are first considered.

Theoretically speaking, the Fourier transform of the corresponding one-dimensional screen should have equal intensity in its zero, ± first, and ± second orders but null intensity in all other diffraction orders. The unit-cell of such a one-dimensional density screen should have a transmittance T(x) of the following form:

$$T(x) = 0.2 + 0.4 \cos(2\pi\, x/X) + 0.4 \cos(4\pi\, x/X) \quad , \tag{1}$$

and

$$T(x) = T(x + X) \quad ,$$

where X is the period of the screen. However, based on nature, the screen cannot have any negative transmittance. Two types of approximations can be made about T(x): 1) Use only the absolute value of T(x), $|T(x)|$, to calculate the spectrum. 2) Set the negative value of T(x) to zero. The transmittance of one unit-cell of the screen and its spatial spectrum is calculated by using a digital computer and the calculated results are plotted. The cell transmission and spectrum for the first type of approximation using $|T(x)|$ are shown in Figures 4 and 5, respectively, and those corresponding to positive values of T(x) are shown in Figures 6 and 7, respectively. By comparing Figures 5 and 7, it can be seen that the approximation with positive T(x) yields more nearly-equal magnitudes in the desired orders. That is, relatively speaking, in this case zero order: first order: second order = 0.264 : 0.183 : 0.154; and the largest higher order is only 0.034.

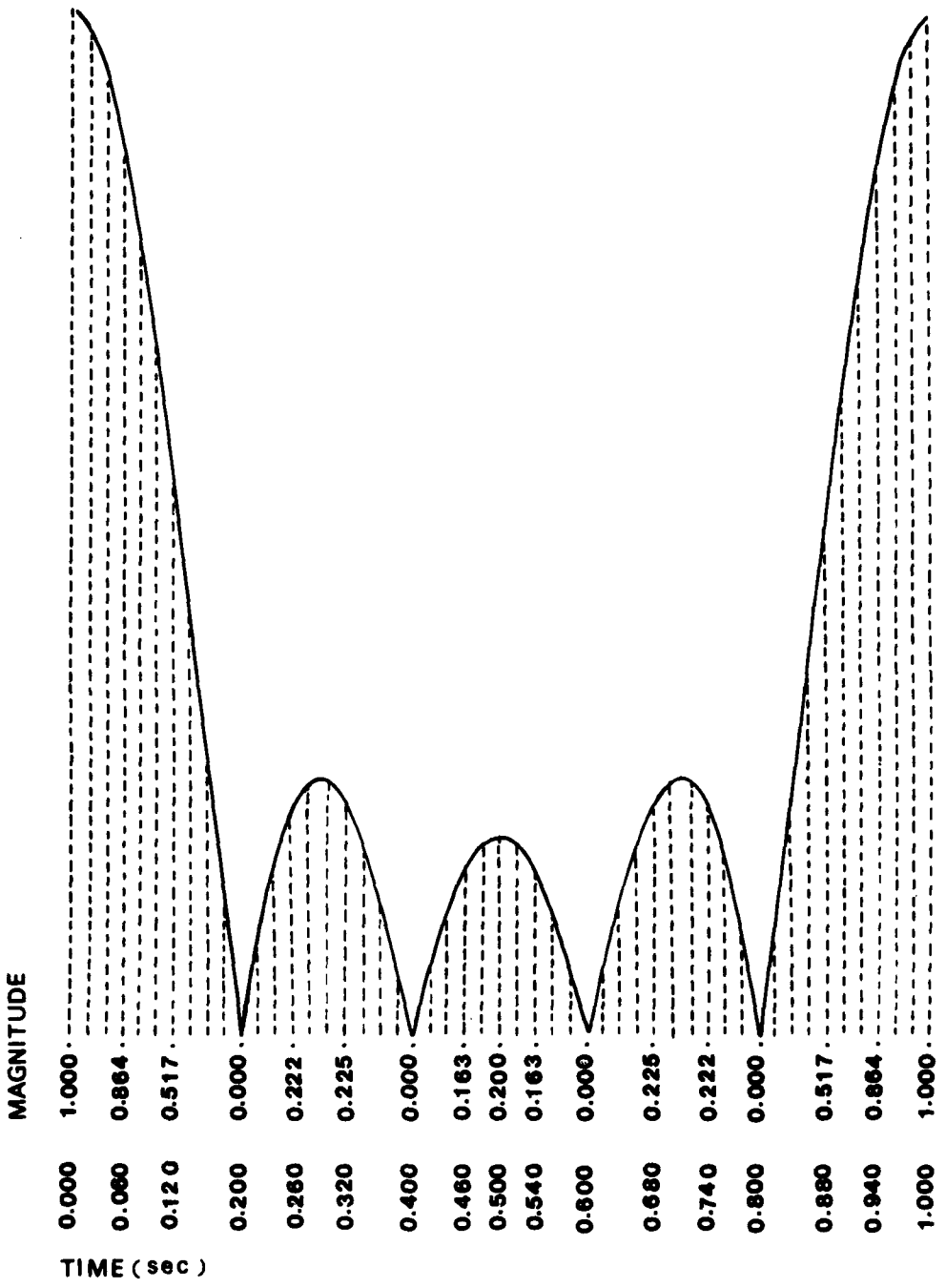

Figure 4. The computer plot of the transmittance $|T(x)|$ of one unit-cell of a one-dimensional contact screen versus x, where $T(x)$ is given by Equation (1).

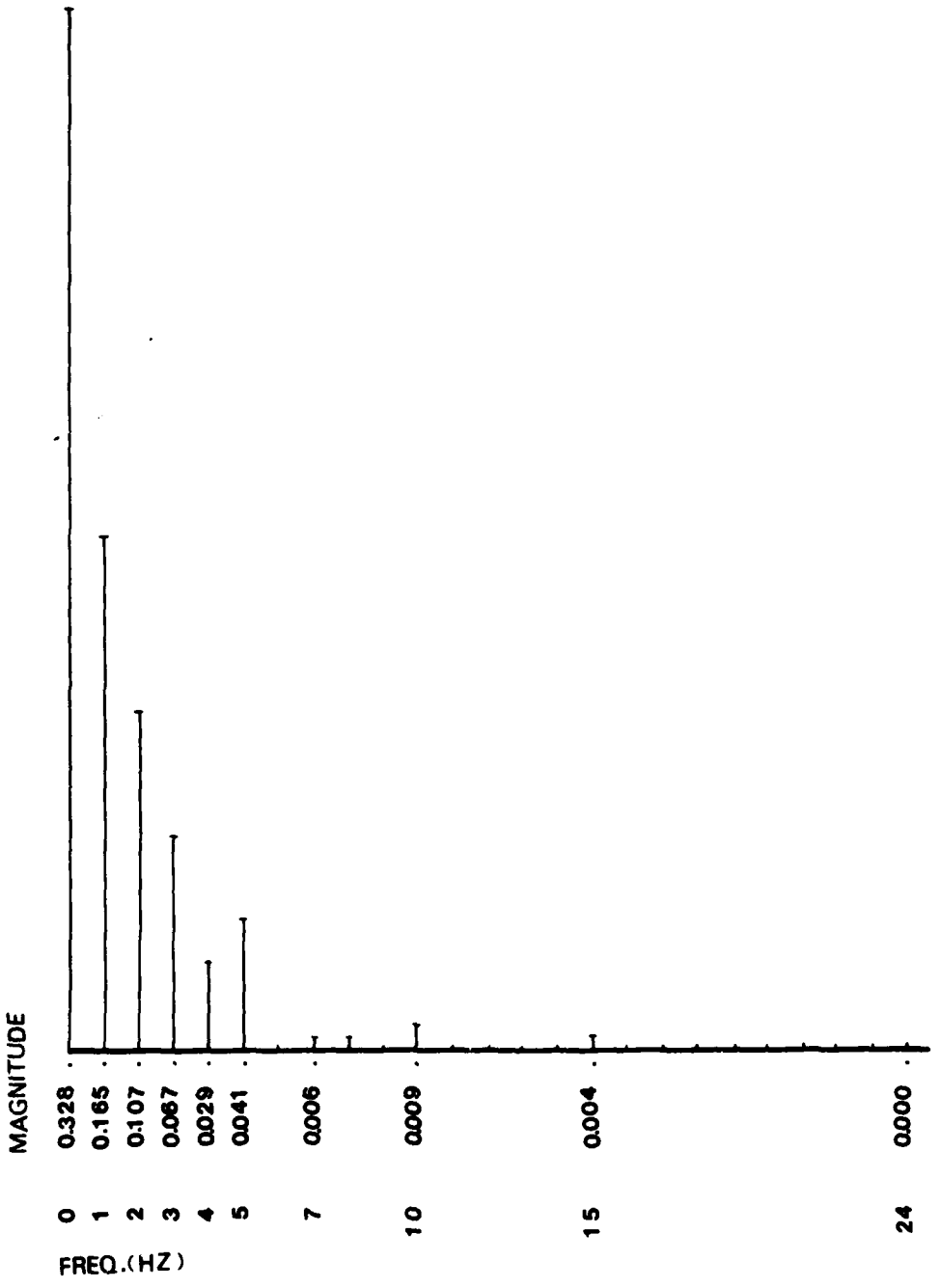

Figure 5. The computer plot of the theoretically calculated Fourier transform of the function $|T(x)|$ of Figure 4 versus spatial frequencies.

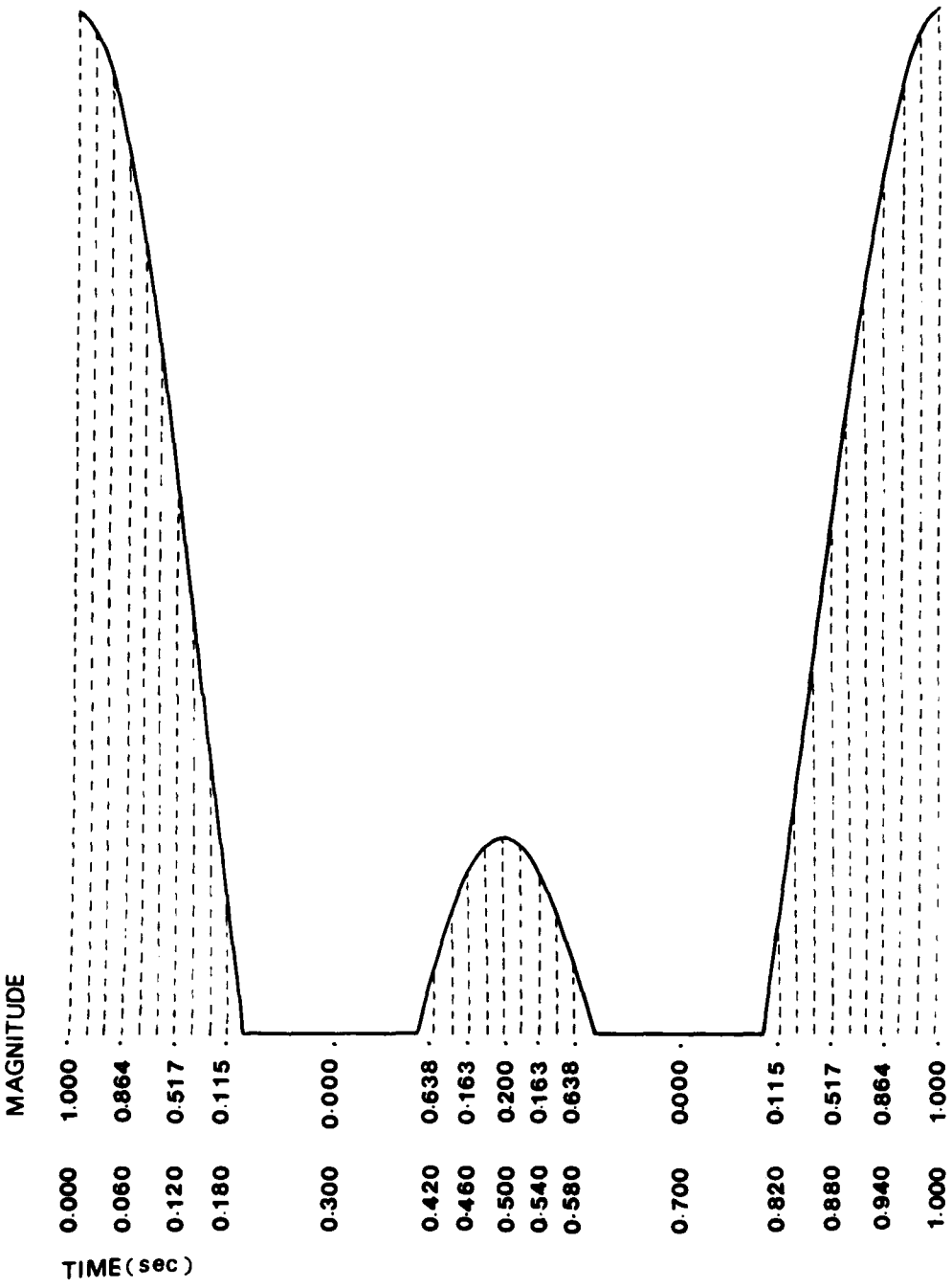

Figure 6. The computer plot of the positive part of the transmittance T(x) of one unit-cell of a one-dimensional contact screen versus x, where T(x) is given by Equation 1.

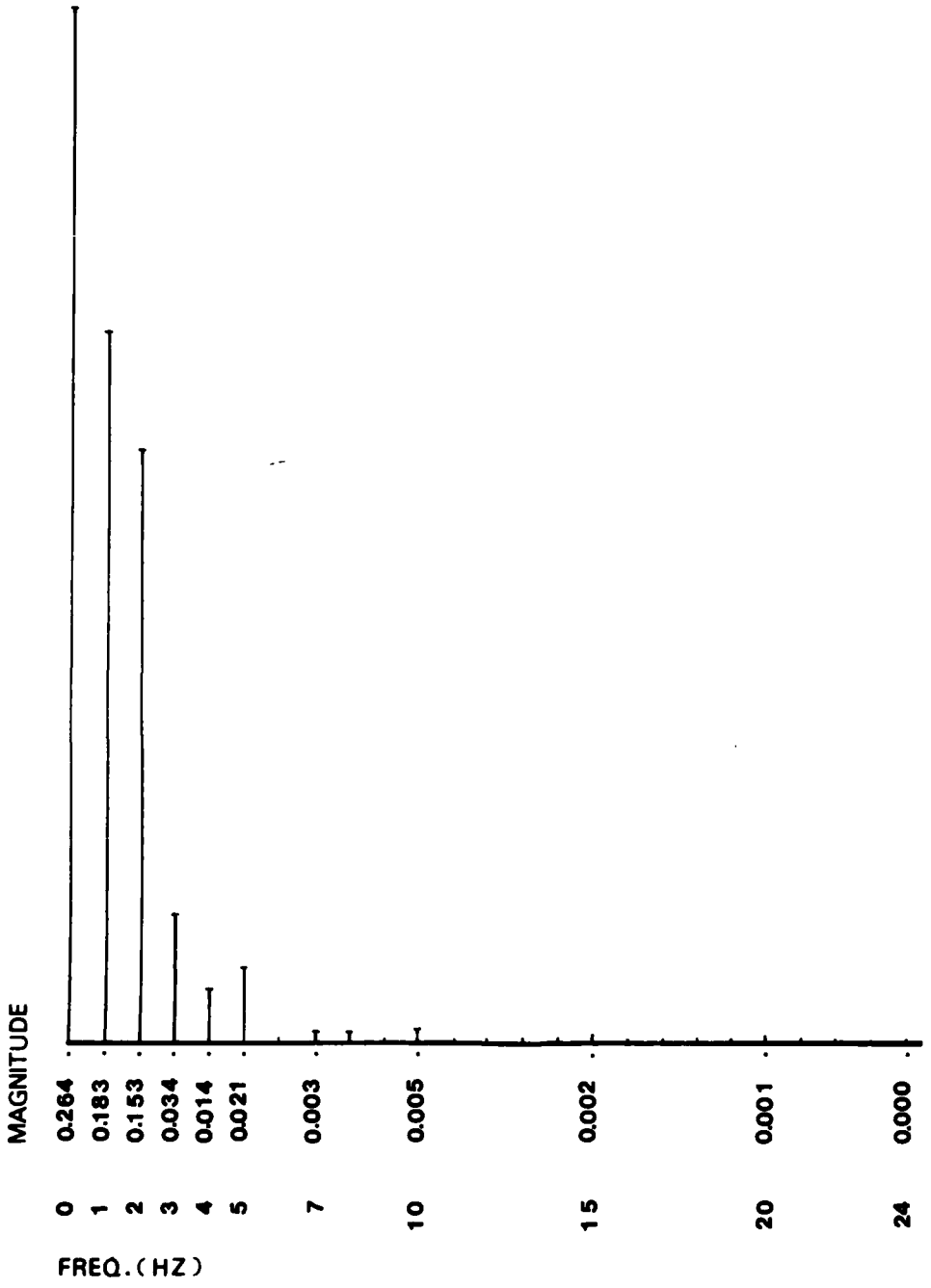

Figure 7. The computer plot of the theoretically calculated Fourier transform of the positive part of the function T(x) of Figure 6 versus spatial frequencies.

Although the cell transmittance distribution of Figure 6 has approximately yielded a result that is close to the desired goal, the actual manufacture of the screen is very difficult. In order to simplify the fabrication of the screen, a further approximation is made. It is assumed that discrete levels of transmittance can be assigned in the screen cell. In case four levels in cell are assumed, the computer plotted cell pattern and its spatial spectrum are shown in Figures 8 and 9, respectively. In this case, the ratio among the lowest three diffraction orders becomes 0.271 : 0.181 : 0.135, and the largest higher order term is 0.045. Apparently this seems not to be a bad approximation. The fabrication of this type of screen will be discussed below.

B. Methods for Screen Fabrication

Two approaches that can be used to fabricate a contact screen are described as follows:

1. Assume there is available a one-dimensional mask which has a periodic intensity transmittance function T(x) of period a, i.e., T(x) = T(x+a), and

$$\begin{aligned} T(x) &= 1 \quad , \quad 0 < x \leqslant a/N \\ &= 0 \quad , \quad a/N < x \leqslant a \quad , \end{aligned} \tag{2}$$

where $N \geqslant 2$.

In the making of the screen, a low-γ negative film is placed below and in close contact with the mask. The film can be made to traverse along the x-direction by means of a translation stage while the mask is fixed. At an initial position of the film, the mask and film are exposed by a uniform incoherent light source for a time τ_1. After the exposure the film is translated along the x-direction for a distance a/N. A second exposure of duration τ_2 is made. The process of stepping a distance a/N and exposing for a time τ_v goes on until the $(N-1)^{th}$ translation and N^{th} exposures are completed. The spatial distribution of exposure becomes

$$E(x) = p\,\tau_i \quad , \quad (i-1)a/N \leqslant x < i\,a/N \quad , \tag{3}$$

where $i = 1,2,\ldots,N$, and p is the local average light power per unit area. If E(x) is located in the linear region of the Hurter-Driffield (H&D) curve, the developed film will have a density distribution D(x) expressed as

$$D(x) = \gamma \log E(x) - D_0 \quad , \tag{4}$$

where γ is the slope of the linear region of the curve, and $-D_0$ is the extrapolated value of density where the straight-line approximation would meet the D-axis. On the other hand, if some of E(x) were in the non-linear region of the H&D curve of the film, Equation (4) can no longer be applied over the whole range. In this latter case, a pre-calibration of the exposures can be used to assure that the desired density levels are achieved. The advantage of the approach described above is that various values of τ_i can be used to shape the periodic density distribution of the contact screen to any predetermined form.

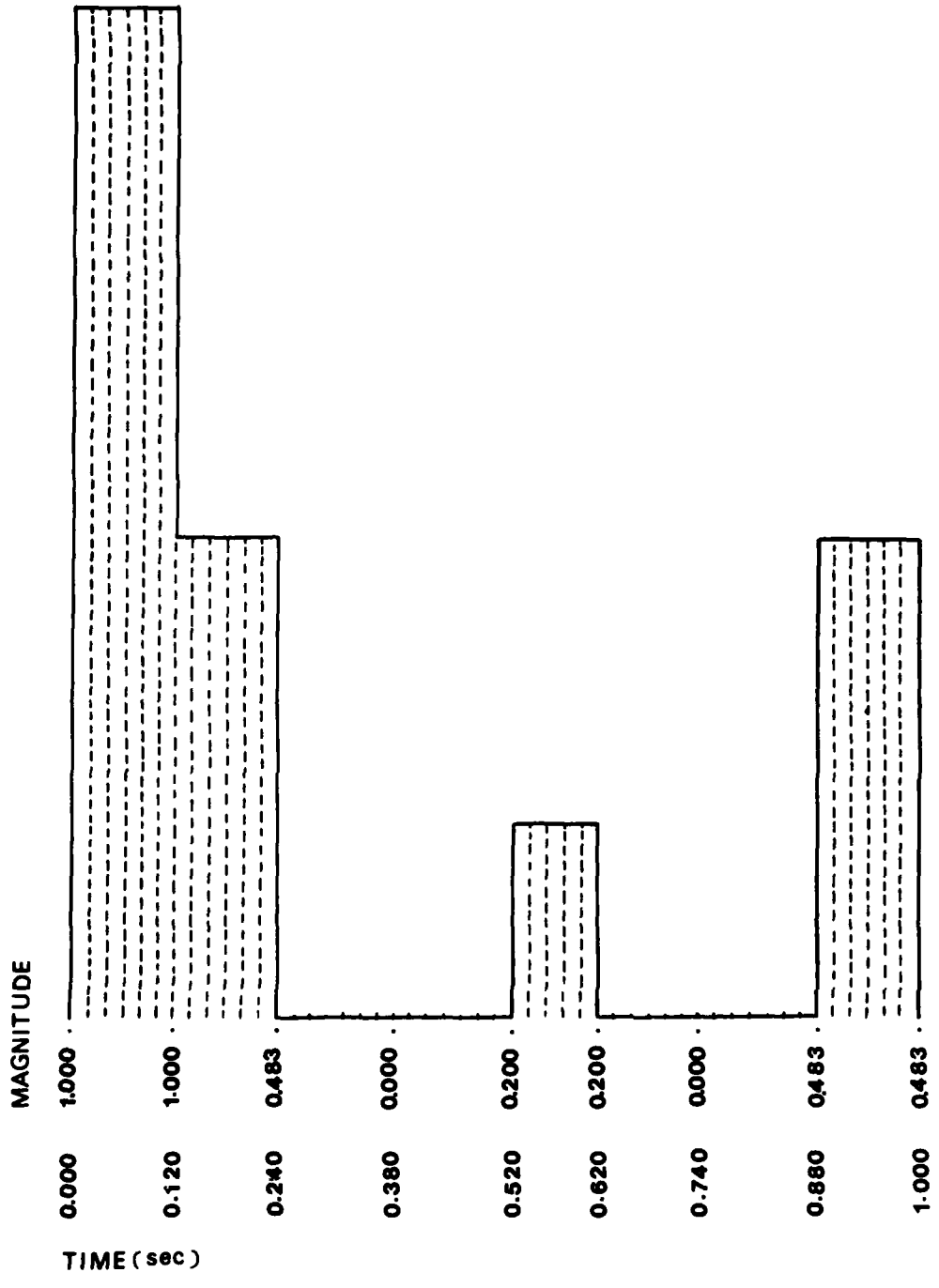

Figure 8. The computer plot of the discrete-valued approximation of the positive part of the transmittance T(x) of one unit-cell of a one-dimensional contact screen versus x, where T(x) is given by Equation (1).

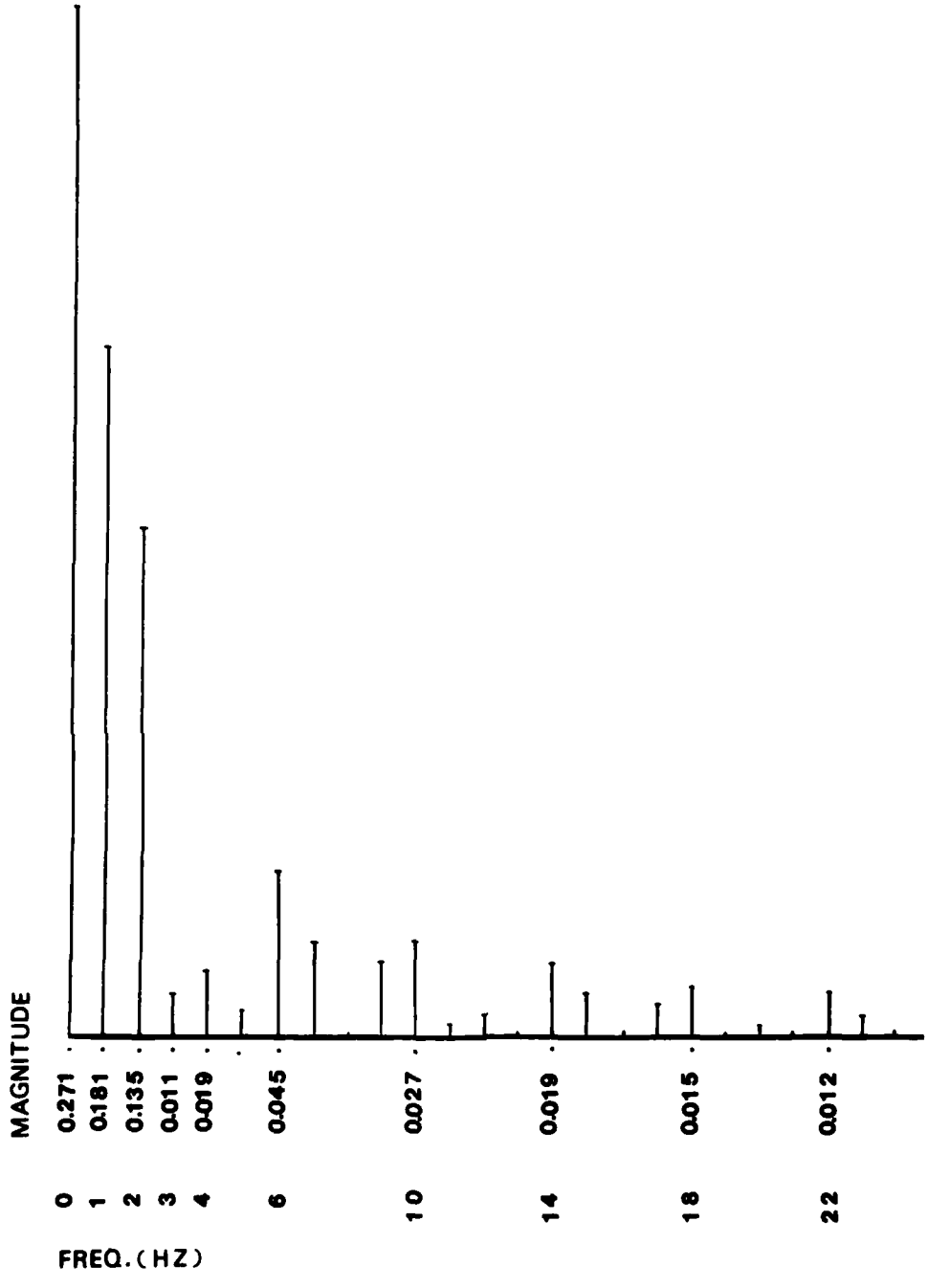

Figure 9. The computer plot of the theoretically calculated Fourier transform of the unit-cell of Figure 8 versus spatial frequencies.

2. If the original one-dimensional periodic mask has an intensity transmittance function T(x), like that of a Ronchi ruling shown in Figure 10(a), it can be described by Equation (2) with N = 2. A different translation-exposure process can now be used in order to obtain a multi-level halftone screen. An example is given in Figure 10, where a three-level screen is generated. With the Ronchi ruling placed in close contact with an Agfa 10E56 photographic plate, a first exposure by an incoherent light source is made. Then the plate is translated an amount $\Delta x = a/3$, and a second exposure is made. After the photographic plate is developed, its density profile will be as shown in Figure 10(c). The three levels of density are $D = D_0$ (fog level), D_1 and D_2. The density profile can be described as

$$
\begin{aligned}
D(x) &= D(x+a) \quad , \quad \text{and} \\
D(x) &= D_1 \quad , \quad 0 < x \leq a/6 \quad \text{and} \\
&\qquad\qquad\quad a/2 < x \leq 2a/3 \quad , \qquad (5) \\
&= D_2 \quad , \quad a/6 < x \leq a/2 \quad , \\
&= D_0 \quad , \quad 2a/3 < x \leq a \quad .
\end{aligned}
$$

The densities D_1 and D_2 are dependent on the exposure and development times used. Even if the exposure times are equal and the exposure is in the linear region, $D_2 \neq 2D_1$ in general, due to the term D_0 in Equation (4). Hence D_1 and D_2 can only be determined either by pre-calibration or by microdensitometer measurement after the fact. The method can be extended to fabricate an N-level screen simply by translating the film plate (N-2) times through a distance a/N for each (N-1) exposure. The density profile of the developed film may be controlled by the exposure times involved.

Both of the approaches described above require relatively unsophisticated equipment. The step size of the screen is controlled by the accuracy of the translation stage.

IV. RESULTS

For the fabrication of the screen with cell transmittance corresponding to Figure 8, the first approach described in III.B.2 has been adopted. A photomicrograph of a few cells of a 133 lines per inch one-dimensional screen is shown in Figure 11 and its Fourier spectrum at the Fourier plane of a lens with focal length of 30 inches is shown in Figure 12. It can be seen that the five spectra islands centered at the zero order are the brightest and are of almost equal magnitude.

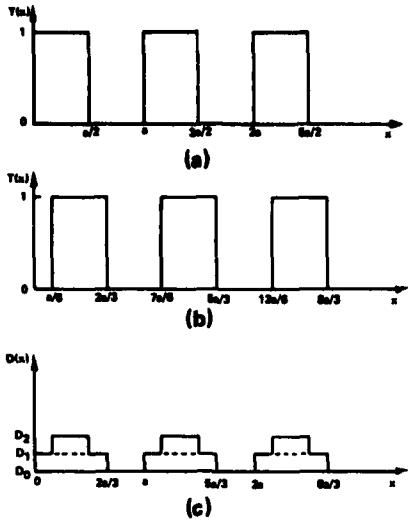

Figure 10. A three-level contact screen produced by one translation of a Ronchi Ruling mask and two exposures.

(a) Ronchi Ruling transmittance function with no translation. The period is a. A first exposure is made at this point.

(b) Ronchi Ruling transmittance with a translation of of the film plate of $\Delta x = a/3$. A second exposure is made at this position.

(c) Density function of the resulted contact screen due to the exposures through the Ronchi Ruling.

A two-dimensional screen is fabricated by repeating the fabrication process of the one-dimensional screen along the two mutually orthogonal directions. The cell patterns of the two-dimensional screen is shown by the photomicrograph in Figure 13. Its corresponding Fourier spectrum is shown in Figure 14. From Figure 14, it can be seen that a 5 x 5 array of almost equal density distribution has been obtained. The measured relative intensity values in μW are shown in the following matrix.

order	-2	-1	0	+1	+2
+2	.35	.35	1.17	.32	.23
+1	.43	.46	1.43	.42	.39
0	.96	.98	2.92	1.01	.91
-1	.48	.40	1.39	.41	.37
-2	.28	.29	1.00	.28	.27

Figure 11. A photomicrograph of a few unit-cells of a specific 133 lpi one-dimensional contact screen.

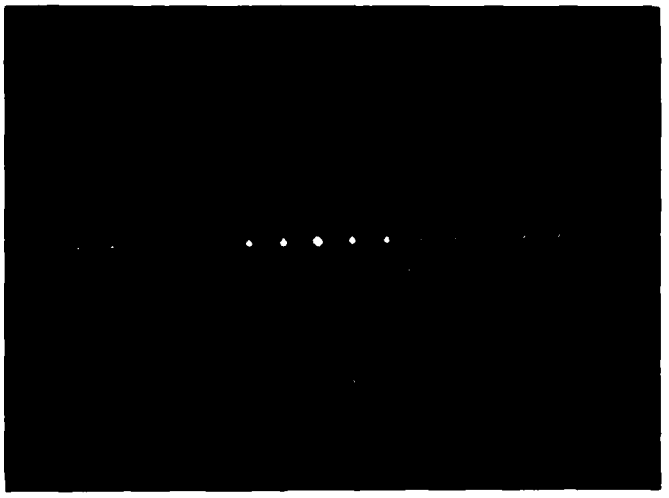

Figure 12. The Fourier transform spatial spectrum of the one-dimensional screen as shown in Figure 11.

Apparently, the various 5 x 5 diffraction orders, including the cross-talk term, are all of the same order of magnitude.

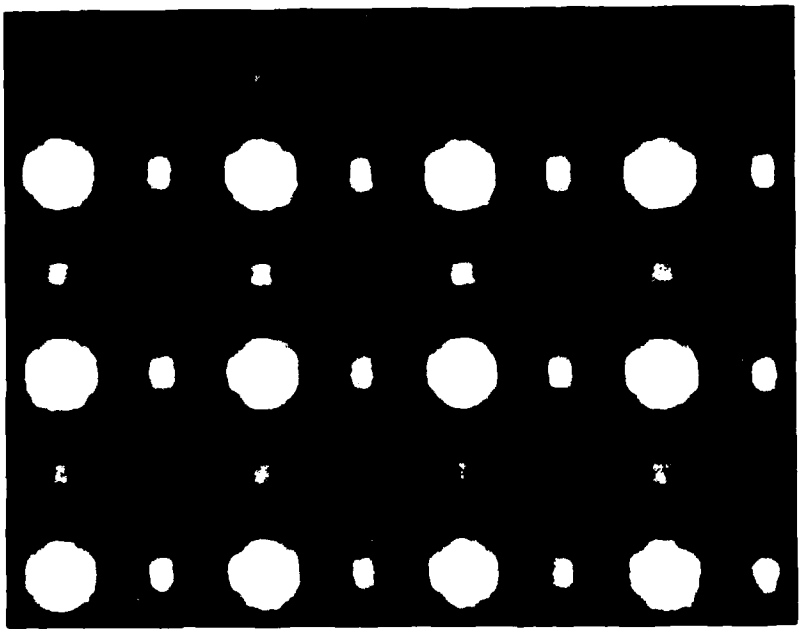

Figure 13. A photomicrograph of a few unit-cells of a two-dimensional contact screen that consists of the superposition of the one-dimensional screen of Figure 11 in two orthogonal directions.

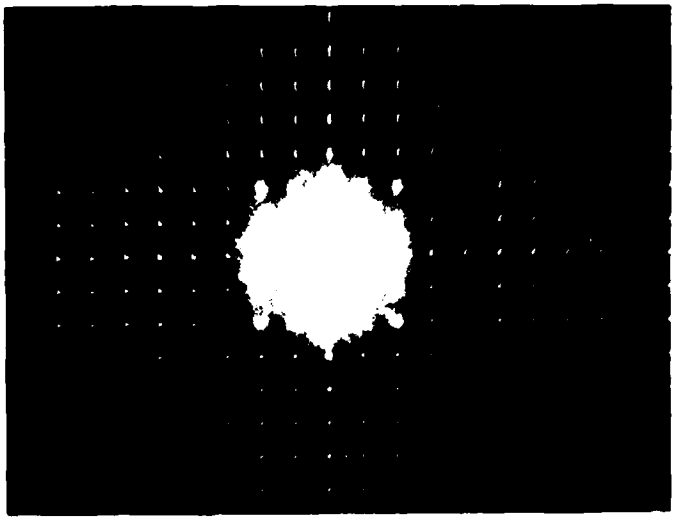

Figure 14. The Fourier transform spatial spectrum of the two-dimensional contact screen as shown in Figure 13.

V. SUMMARY AND DISCUSSION

One- and two-dimensional density-type contact screens have been designed and fabricated for application in a real-time matched filter correlator. The spatial Fourier transform of the two-dimensional screen has a 5 x 5 array of spectra islands where most of the energy in the light beam are distributed among them. The measured individual light intensity of each of these 25 spectra islands, though not equal to one another, is approximately on the same order of magnitude as any others. However, the major problem of the density-type contact screen is that it suffers significantly from the loss of light efficiency. The efficiency loss occurs due to the absorption of light by the silver particles in the screen.

One method of remedying the loss of light efficiency is to make a phase contact screen in a dichromated gelatin material. How to exactly control the phase values in the unit-cells of the screen so that a phase screen which can yield a 5 x 5 array of spectra islands of approximately equal intensity will need further theoretical and experimental investigations. It seems to be almost certain from preliminary investigations that a perfect 5 x 5 evenly-distributed array of spectra islands probably can never be obtained from the screen due to practical experimental difficulties. Nevertheless, it is expected that an array which is close enough to the ideal one can be obtained.

Once a nearly ideal screen is obtained, it can be used in the system for auto-correlation experiment. The screen can also be used in a solid-state laser correlator at wavelength of 820 nm when the filter is recorded at the He-Ne wavelength. This requires that the matched filter be recorded with distances between the islands of the spectra array scaled to fit for the solid-state laser (or any other intended lasers) wavelength. The image should also be scaled through a zoom lens or by placing it at a proper location in the system.

DISTRIBUTION

	No. of Copies
Commander US Army Research Office ATTN: DRXRO-PH, Dr. R. Lontz P. O. Box 12211 Research Triangle Park, NC 27709	5
US Army Research and Standardization Group (Europe) ATTN: DRXSN-E-RX/LTC D. R. Reinhard Box 65 FPO New York 09510	1
Commander US Army Materiel Development and Readiness Command ATTN: Dr. James Bender Dr. Gordon Bushey 5001 Eisenhower Avenue Alexandria, VA 22333	1 1
Headquarters, Department of the Army Office of the DCS for Research, Development & Acquisition ATTN: DAMA-ARZ Room 3A474, The Pentagon Washington, DC 20301	1
OUSDR&E Room 3D1079, The Pentagon Washington, DC 20301	1
Director Defense Advanced Research Projects Agency 1400 Wilson Boulevard Arlington, VA 22209	1
OUSDR&E ATTN: Dr. G. Gamota Deputy Assistant for Research (in Advanced Development) Room 3D1067, The Pentagon Washington, DC 20301	1
Director of Defense Research and Engineering Engineering Technology Washington, DC 20301	1
Director Defense Advanced Research Projects Agency/STO ATTN: Commander T. F. Wiener D. W. Walsh 1400 Wilson Boulevard Arlington, VA 22209	1 1

Commander
US Army Aviation Systems Command 1
12th and Spruce Streets
St. Louis, MO 63166

Director
US Army Air Mobility Research & Development Laboratory 1
Ames Research Center
Moffett Field, CA 94035

Commander
US Army Electronics Research & Development Command
ATTN: DRSEL-TL-T, Dr. Jacobs 1
DELEW-E, Henry E. Sonntag 1
Fort Monmouth, NJ 07703

Director
US Army Night Vision Laboratory
ATTN: John Johnson 1
John Deline 1
Peter VanAtta 1
Fort Belvoir, VA 22060

Commander
US Army Picatinny Arsenal 1
Dover, NJ 07801

Commander
US Army Harry Diamong Laboratories 1
2800 Power Mill Road
Adelphi, MD 20783

Commander, US Army Foreign Science & Technology Center
ATTN: W. S. Alcott 1
Federal Office Building
220 7th Street, NE
Charlottesville, VA 22901

Commander, US Army Training & Doctrine Command
Fort Monroe, VA 22351 1

Director, Ballistic Missile Defense Advanced Technology Center
ATTN: ATC-D 1
ATC-O 1
ATC-R 1
ATC-T 1
P. O. Box 1500
Huntsville, AL 35808

Commander, US Naval Air Systems Command
Missile Guidance and Control Branch 1
Washington, DC 20360

Chief of Naval Research Department of the Navy Washington, DC 20301	1
Commander US Naval Air Development Center Warminster, PA 18974	1
Commander, US Naval Ocean Systems Center Code 6003, Dr. Harper Whitehouse San Diego, CA 92152	1
Director, Naval Research Laboratory ATTN: Dave Ringwolt Code 5570, T. Gialborinzi Washington, DC 20390	1 1
Commander, Rome Air Development Center ATTN: James Wasielewski, IRRC Griffiss Air Force Base, NY 13440	1
Commander, US Air Force, AFOSR/NE ATTN: Dr. J. A. Neff Building 410, Bolling Air Force Base Washington, DC 20332	1
Commander, US Air Force Avionics Laboratory ATTN: D. Rees W. Schoonover Dr. E. Champaign Dr. J. Ryles Gale Urban David L. Flannery Wright Patterson Air Force Base, OH 45433	1 1 1 1 1 1
Commander, AFATL/LMT ATTN: Charles Warren Eglin Air Force Base, FL 32544	1
Environmental Research Institute of Michigan Radar and Optics Division ATTN: Dr. A. Kozma Dr. C. C. Aleksoff Juris Upatnieks P. O. Box 8618 Ann Arbor, MI 41807	1 1 1
IIT Research Institue ATTN: GACIAC 10 West 35th Street Chicago, IL 60616	1
Dr. J. G. Castle 9801 San Gabriel, NE Albuquerque, NM 87111	1

Commander, Center for Naval Analyses 1
ATTN: Document Control
1401 Wilson Boulevard
Arlington, VA 22209

Dr. J. W. Goodman
Information Systems Laboratory 1
Department of Electrical Engineering
Stanford University
Stanford, CA 04305

Eric G. Johnson, Jr.
National Bureau of Standards 1
325 S. Broadway
Boulder, CO 80302

Dr. Nicholas George
The Institute of Optics 1
University of Rochester
Rochester, NY 14627

Naval Avionics Facility
Indianapolis, IN 46218 1

Dr. David Cassasent
Carnegie Mellon University 1
Hamerschage Hall, Room 106
Pittsburg, PA 15213

Professor Anil K. Jain
Department of Electrical Engineering 1
University of California, Davis
Davis, CA 95616

Terry Turpin
Department of Defense 1
9800 Savage Road
Fort George G. Meade, MD 20755

Dr. Stuart A. Collins 1
Electrical Engineering Department
Ohio State University
1320 Kennear Road
Columbus, OH 43212

US Army Materiel Systems Analysis Activity 1
ATTN: DRXSY-MP
Aberdeen Proving Ground, MD 21005

US Army Night Vision Laboratory
ATTN: DELNV-L, Dr. R. Buser 1
Fort Belvoir, VA 22060

Dr. F. T. S. Yu
Penn State University 1
Department of Electrical Engineering
University Park, PA 16802

Dr. William P. Bleha
Liquid Crystal Light Valve Devices 1
Hughes Aircraft Company
6155 El Camino
Carlsbad, CA 92008

DRCPM-PE-E, Mr. Pettitt 1
-PE 1

DRSMI-LP, Mr. Voigt 1
-O 1
-Y 1
-R 1
-RN, Mr. Hagood 1
-RE, Mr. Pittman 1
-RD 3
-RG 1
-RG, Mr. McLean 1
-RR, Dr. Hartman 1
Dr. Bennett 1
Dr. Christensen 1
Dr. Duthie 80
-RPR 15
-RPT, Record Copy 1


FILMED
9 8